INTERNATIONAL JOURNAL OF
COASTAL, OFFSHORE & ENVIRONMENTAL ENGINEERING
IJCOE Vol.11/No. 3/Summer 2026 (86-97)

Available online at: www. Ijcoe.org

The failure probability of reinforced concrete marine structures and cost optimization of maintenance

Abdolhossein Mohammadrahimi[1*], Afshin Ghasri[2], Mesbah Sayebani[3], Akbar Esfandiari[4]

[1*] *Assistant Professor,Department of Marine Engineering, Chabahar maritime university, Shahid Rigi Ave, Chabahar, Iran; rahimi@cmu.ac.ir*
[2] *Department of Maritime Engineering, Amirkabir University of Technology, Hafez Ave, Tehran, Iran; afshin;ghasri@gmail.com*
[3] *Assistant Professor, Department of Maritime Engineering, Amirkabir University of Technology, Hafez Ave, Tehran, Iran; msaybani@aut.ac.ir*
[4] *Assistant Professor,Department of Maritime Engineering, Amirkabir University of Technology, Hafez Ave, Tehran, Iran; a_esfandiari@aut.ac.ir*

ARTICLE INFO

Article History:
Received 2 Apr 2026
Accepted 15 July 2026
Available online ….

Keywords:
Corrosion, Crack width, symptom-based Reliability, Maintenance and repair, Cost Optimization

ABSTRACT

Due to the increased life of marine structures in the world, repair and maintenance of low cost and high reliability are of concern in this industry. In this paper, the corrosion-induced crack width of reinforced concrete (RC) structure in the marine environment is estimated according to the experimental data, laboratory results, and numerical formulas. Symptom-based Weibull function distribution and Bayesian theory have been used to predict the structural reliability in different modes (without repair and maintenance, with maintenance, and with repair and maintenance) and the probability of failure was assessed before and after maintenance to predict the appropriate time for its implementation using Bayesian theory. Bi-objective optimization was utilized to provide the client with optimal decisions regarding the probability of structural failure as well as the type of repair and maintenance strategies. The results showed the effectiveness of the proposed method in predicting performance, improving life service, and optimizing repair and maintenance costs of the marine structure.

1. Introduction

Improving marine structure lifetime is a recent concern for maritime industry in the word. Marine structures are being under serious damage or even severe failure as they are subjected to the environmental forces of aggressive marine environment including corrosion, waves, floats, etc. The evident need for effective repair and maintenance strategies is felt by all concerned in maritime industry including owners, classification society, and officials. Repair and maintenance are more cost-effective, less risky, and simpler than the design and construction of marine structures. This need is more evidently felt when the structure service age is increased [1].

Structural health monitoring is one of the ways to identify fatigue damage to the structure. Its ultimate goal is to detect the existence, location, and extent of structural damage. Additional to structural health monitoring and its data, reliability and probabilistic analysis can be utilized to predict future performance and service life of the structure. The durability of the structure is enhanced using repair and maintenance strategies to improve structural performance and lifetime. A targeted program can provide information on the present condition, repair and maintenance regularities, and the future performance of the structure.

Full inspection and assessment are requisites to ensure the sustainability of structure and reduce costs (proper repair and maintenance implementation). Structural health monitoring strategy is integrated with life cycle management to predict the structure performance, estimate optimal maintenance strategy, and thus use the structure beyond its design life span. RC structures as a type of marine structures may change from the initial design to the state that threatens their safety and usability due to corrosion, service aging, or changes in their resistance to toughness. Therefore, damage prediction is essential to estimate the structure remnant life and implement maintenance and repairs. In fact, the structural reliability and serviceability are predictable from probabilistic functions using specific information of structures (crack width in RC structures). The prediction of future state from observation of present state via probabilistic functions determines a set of actions to optimize repair and maintenance strategies based on the structural reliability and costs.

.

In this paper, data from various experimental resources and results from computational relations on crack width estimation in the marine environment are used to predict the probability of failure and the remaining life of RC structures by the use of Weibull function distribution. Assuming that repair and maintenance service has been done, the structure information is updated and the probabilistic functions are analyzed by means of Bayesian theory. Finally, the information obtained from probability functions in different modes is used to estimate the optimal choice based on time and cost for repair and maintenance of the structure.

There have been various assessments of cracking and its impact upon structural fracture. Recent research shows that life expectancy of RC structures is highly dependent on environmental conditions. The corrosive atmosphere is a determinant of corrosion and cracking in RC structures [2,3]. There is sample research on the problem of concrete corrosion and surface cracking that predict theoretical models for its developing time [4–7]. Some researchers have modeled fatigue behavior adapting the finite element method to contrast the laboratory with model data for the structure [8–10]. In addition, various mathematical models have been proposed to predict concrete cracking time [11]. In the past, some research has been done on crack development in RC structures. Liu and Weyers first modeled the time to steel corrosion-induced cracking on cover concrete in a round of experiments. They made 5-year observations on the distribution of model cracks to examine the impact of corrosion on reliability. They found that cracking time acts as a symptom of the time-based prediction model [5].

The science of reliability is willingly introduced in the 1960s. Some probabilistic methods have been used to predict the structure's lifetime. These methods can predict a more accurate and realistic life span and time to corrosion at cracked surfaces [12–15]. In 1968, Benjamin proposed the concept of probabilistic design and structural reliability [16]. In 1987, Frangopol et al. examined the effect of structural damage on time-based reliability [17]. In 1998, Sarma and Adeli conducted a study on RC structures suggesting that the focus of research must shift from the initial optimization cost to the repair and maintenance costs [16].

In 1983, Surahman and Rojiani developed reliability-based optimizations for RC structures [16]. In 2000, Cempel et al. introduced a new concept of reliability based on symptoms (physical properties) to assess system conditions. This reliability has priority over time-based reliability in updating useful data (physical properties) to assess the structure's current and future conditions. Later, this concept of reliability was applied to measurable data such as geometry, material properties, static and dynamic behavior, structural damage and loading [18]. In 2011, Straub designed a new method to estimate the reliability of RC structures using Bayesian theory [19].

In 2012, Chen and Alani evaluated reliability to calculate offshore structure deterioration over time, providing an optimal repair program for the structure service life [20]. In 2015, Chen investigated the effect of corrosion on RC structures in an experimental research based on physical properties. The crack width of steel-concrete bond corrosion was studied using reliability based on physical properties on which the data were collected. Weibull probability distribution and Bayesian updating functions were used to assess reliability and predict the best repair and maintenance time to extend service life of the structure [21].

In 2017, Yu Bo et al. investigated the impact of sea environment on the reliability and probability of failure in offshore RC structures. They also examined environmental conditions, material properties, parameters influencing RC structures, and their implementation in the marine environment [21].

2. Corrosion in the Marine Environment

2.1. Initiation and Propagation of Cracks

corrosion cracking that leads to the failure of marine structures containing high-strength steel occurs in three different phases.

1) Crack initiation , 2) Crack propagation at a slow rate, 3) Fully cracked cover at a high propagation rate approaching the critical condition and leading to the final fracture [22].

The crack width on the concrete cover surface as an on-site measurable parameter follows analytical models. Experimental research shows that the bond strength of corroded steel is highly correlated with the crack width of concrete. The bond strength can be expressed as a function of crack width over time [23]. Figure 1 shows the predicted bond strength of intact normalized steel [24] and the experimental result of Law et al. [25].

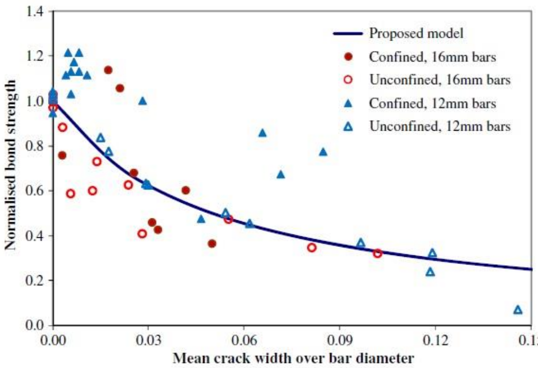

Figure 1. Normalized bond strength as a function of the ratio of mean crack width over the steel bar diameter, analytical predictions and experimental results of Law et al. [26]

As the bond strength of corroded steel decreases, the structure load-bearing capacity like bending strength is decreased. The results indicate that crack width is a predictor of steel bond strength. The reduction in bond strength begins with the initiation of concrete cover cracking. Therefore, crack width can be considered as a proper symptom in assessing the probability of failure and the reliability of the structure. The data on crack width can be used to estimate the structure remaining life.

2.2 Corrosion-induced Cracking Model

Steel corrosion-induced concrete cracking can be modeled as a walled cylinder, as shown in Figure 2 [26]. In this model, rebar with an internal radius of D_b is located in a clear concrete cover C. The first damage occurs on the concrete surface [27].

Diagrams must be also represented with clear axes, fonts, without background, with distinguishable lines in a black and white version.

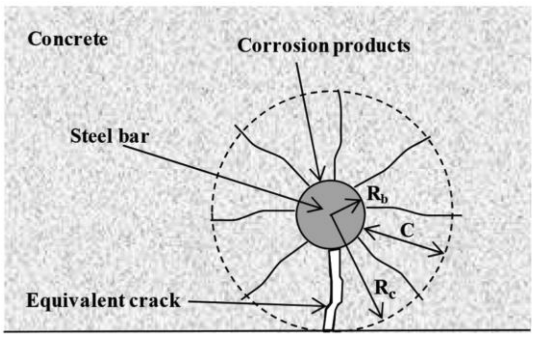

Figure 2. Schematic of steel-concrete bond corrosion [27]

The mass of rust (M_r) produced (Kg/m) per unit time is expressed as Eq.(1) [28]. Using this equation, the rate of corrosion rust in a period of time can be easily calculated.

$$M_r = \left(m_c \int_0^t \pi D_b i_{corr}(\tau) d\tau\right)^{1/2} \quad (1)$$

In this equation, t is the duration of corrosion per year, m_c is an empirical coefficient taken as 2.1×10^{-2}, i_{corr} represents the mean annual corrosion current per unit length at the surface area of the rebar [28].

2.2.1. Crack Initiation

The mass of rust produced at the beginning of cracking is calculated by Eq.(2) [28]:

$$M_r(T_p) = \frac{\pi}{\alpha_m} D_b d_0 \quad (2)$$

T_p is the time required for corrosion products to fill a porous zone of thickness d_0.

The parameter α_m is an empirical coefficient taken as $\alpha_m = 2.05 * 10^{-4}$ [28]. In other words, the time required to fill the entire porous zone (T_p) can be estimated using Eq.(1). It is also worth noting that rust propagation causes stress in rebar surroundings. Therefore, when the hoop stress at the rebar surface equals the tensile strength, the concrete initiates to crack at the rebar surface. The required mass of rust is obtained by Eq.(3) [28]:

$$M_r(T_i - T_p) = \frac{(1-\upsilon)R_b^2 + (1+\upsilon)R_c^2}{R_b^2 + R_c^2} \times R_b \times \frac{f_t}{E} \times \frac{\pi D_b}{\alpha_m} \quad (3)$$

R_b represents the radius of the reinforcement, R_c represents the corrosion radius of the concrete surface, υ is the Poisson's coefficient, E is Young's modulus, f_t corresponds to the tensile strength and T_i is the time required for corrosion to be started.

Similarly, the required time for crack initiation at the rebar surface is calculated from the time through which the porous zone is filled to the time through which hoop stress approaches the tensile strength (Eq.(1)). In these equations, corrosion time and rate in marine environment are calculated based on the structure geometric properties until crack propagation.

2.2.2. Crack Propagation

Numerous studies have been carried out on concrete cracking models that indicate no significant change in concrete deterioration under different conditions [29]. On the other hand, a significant increase in the crack width is associated with an insignificant tensile strength of cracked concrete.

The normalized actual crack width in $W(r)$ is defined as follows [28]:

$$W = \frac{f_t}{G_F} w(r) \quad (4)$$

where G_F is the fracture energy of concrete.

The normalized crack width is revised as follows [28]:

$$W = \frac{\delta_{bc}(R_c . r)}{\delta_{bc}(R_c . R_b)} W_b \quad (5)$$

In this equation, the crack width coefficient $\delta_{bc}(R_c.r)$ is expressed as follows and the coefficient $\delta_{bc}(R_c.R_b)$ is obtained from $\delta_{bc}(R_c.r)$ when $r = R_b$.

$$\delta_{bc}(R_c.r) = \frac{(R_c - r)}{l_0(l_0 - R_c)(l_0 - r)} + \frac{1}{l_0^2} ln \frac{R_c|l_0 - r|}{r|l_0 - R_c|} \quad (6)$$

where $l_0 = \frac{n_c W_{cr}}{2\pi} l_{ch}$ and $l_{ch} = \frac{E\, G_F}{f_t^2}$, $n_c = \frac{2\pi R_c}{L_c}$.

l_{ch} is the length of property introduced by Hillerborg et al. [30] and L_c is the spacing of crack bands [28].

Therefore, the normalized crack width at rebar surface W_b is expressed as follows:

$$W_b = ((1+\nu)R_c(l_0 - R_c)\delta_{bc}(R_c.R_b) \times W_{cr}) \quad (7)$$

The mass of rust required for the crack propagation on the concrete surface at the time of crack initiation is obtained by Eq.(8):

$$M_r(T_c - T_p) = [1 + \frac{l_0 - R_b}{R_b} \frac{W_b}{W_{cr}}] \times R_b \times \frac{f_t}{E} \times \frac{\pi\, D_b}{\alpha_m} \quad (8)$$

As a result, the time for the crack to propagate on the concrete surface T_c is estimated using Eq.(1).

2.2.3. Fully Cracked Cover

As soon as cracking reaches the surface of free concrete, the cover is completely cracked. The normalized crack width at this stage of corrosion is expressed as bellow [28]:

$$W = W_c + \frac{\delta_{bc}(R_c.r)}{\delta_{bc}(R_c.R_b)}(W_b - W_c) \quad (9)$$

The normalized crack width at the rebar surface W_b within the time period of this stage is also expressed as bellow [28]:

$$W_b = \left(\frac{E}{f_t} \times \frac{\alpha_m M_r(t)}{\pi\, D_b} - R_b\right) \times \frac{W_{cr}}{l_0 - R_b} \quad (10)$$

Therefore, the crack width at the concrete surface W_c can be calculated as a function of time. The time to reach the critical value for concrete T_{cr} can be estimated by Eq.(10) assuming that $W_b = W_{cr}$. Also, the critical mass of rust (concrete surface cracking) can be calculated by Eq.(11):

$$M_r(t_{cr}) = \frac{l_0 f_t D_b\, \pi}{E\, \alpha_m} \quad (11)$$

Finally, if i_{corr} is kept constant during the cracking process, the total crack width per time t is the sum of all concrete surface crack widths [31]. Therefore, the crack width is considered as a function of time as follows [28]:

$$\begin{aligned} &\tilde{w}(t) = 0 && for\ 0 \le t \le T_c \\ &\tilde{w}(t) = a^c t^{1/2} - b^c && for\ T_c \le t \le T_{cr} \\ &\tilde{w}(t) = a^d t^{1/2} - b^d && for\ t > T_{cr} \end{aligned} \quad (12)$$

The values of a^c and b^c can be represented as below:

$$a^c = 0.145\, \alpha_m \frac{E}{f_t} \sqrt{\frac{i_{corr}}{\pi\, D_b}} \times \frac{1}{(l_0 - R_b)[1 - R_c(l_0 - R_c)\delta_{bc}(R_c.R_b)]} \times n_c W_{cr} \quad (13)$$

$$b^c = \frac{\frac{R_b}{(l_0 - R_b)} + R_c(l_0 - R_c)\delta_{bc}(R_c.R_b)}{1 - R_c(l_0 - R_c)\delta_{bc}(R_c.R_b)} \times n_c W_{cr} \quad (14)$$

Also, the values of a^d and b^d can be represented as below:

$$a^d = 0.145\, \alpha_m \frac{\sqrt{\pi\, D_b i_{corr}}}{R_{cr}} \quad (15)$$

$$a^d = \pi\, D_b \left(1 - \frac{R_b}{R_{cr}}\right) - n_c W_{cr} \quad (16)$$

Therefore, it can be concluded that if the mean corrosion rate of rebar remains constant during the process, the crack propagation induced by steel corrosion follows square–root–of–time rule.

2.3. Sample Beam

A concrete beam in the marine environment is considered as the study structure in this paper. The beam includes a rebar of 16 mm diameter with a clear concrete cover of 40 mm. The mean compressive strength of concrete is taken f_c = 45 MPa. This value is also considered to estimate other properties of concrete. Therefore, the required parameters are estimated as follows:

The tensile strength of concrete is equal to $f_t = 0.69\sqrt{f_c} = 4.63\ MPa$

The modulus of elasticity is equal to $E = 4400 f_c^{0.516} = 31.4\ GPa$

Poisson's coefficient is taken as ν = 0.18

According to laboratory data, the fracture energy of concrete and the ultimate cohesive crack width are respectively considered $G_F = 96\ N/m$ and $w_u =$

$0.15\ mm$ in the structure. According to previously used data [28,31], the allowable crack width is assumed to be $w_l = 1\ mm$ for the RC structure in the marine environment. Also, the maximum aggregate size is considered to be 25 mm. The total crack number is obtained from the formula $n_c = 2\pi\ R_c/L_c \approx 4$. The structure designed service life is 60 years. Also, the baseline of the corrosion penetration rate is $i_{corr} = 5\ \mu A/cm^2$.

The crack width per unit time has been calculated by some methods and the crack growth in RC structures has been formulated by some researchers. Alongside crack growth prediction, different laboratory data [27,32–34] have been collected by Chen [24]. In the following, the Eq.(12) is used to predict the cracked structure width (with studied specification). As shown in Figure 3, there is no significant difference between predicted data by Eq.(12) and predicted data by Chen in the corrosion-induced crack width. These results are taken as the presumptions for the crack growth in the offshore environment and used for the following predictions.

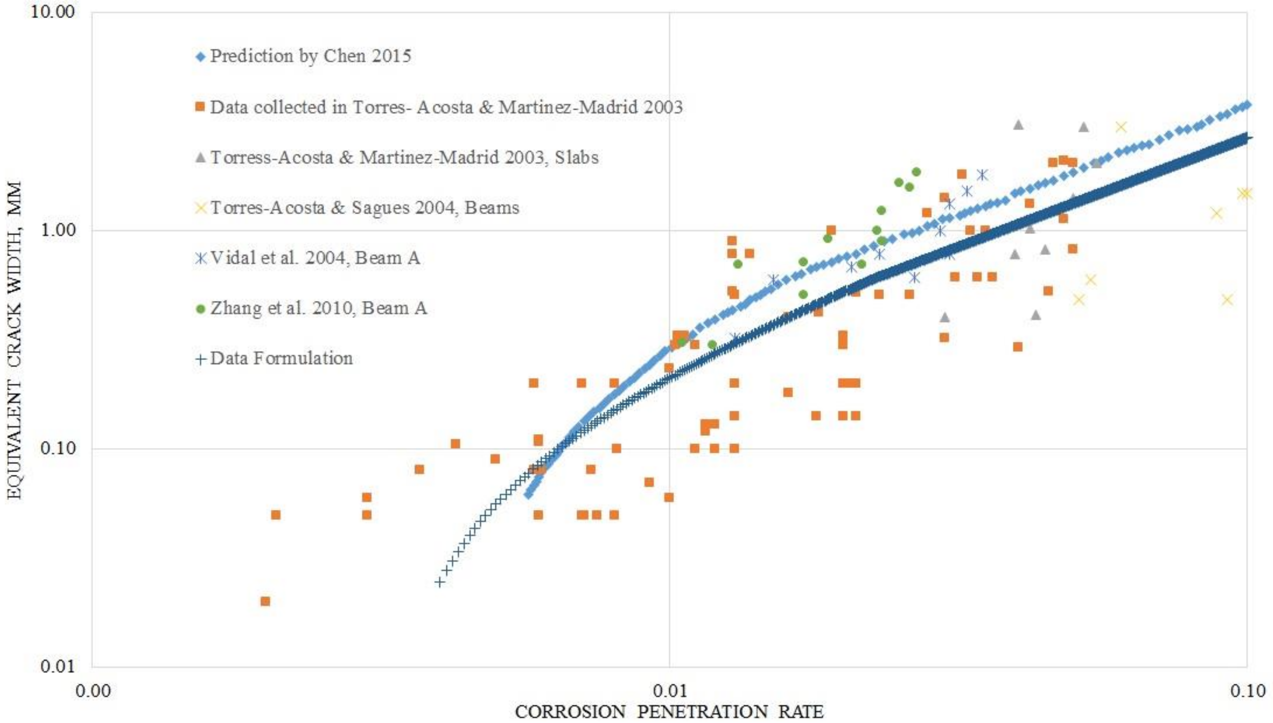

Figure 3. Crack width values under the function of mean corrosion penetration rate (laboratory data and presumed results)

3. Symptom-based Reliability and Weibull Function Distribution

Time-based reliability is an old method that has given way to symptom-based reliability due to some limitations including ignorance of extra information available to the structure. Since environmental forces are constantly changing in the specific maritime environment, symptom-based reliability has priority over time-based reliability for marine structures. The health monitoring process can formulate useful symptoms to evaluate the current state and predict the future condition for developing optimal maintenance strategies. In symptom-based systems, reliability depends on measurable data. When a symptom exceeds its critical value, the failure of system or its components will take place [18]. Weibull model as a well-known and flexible model for service life distribution can be used for symptom-based reliability. Therefore, in Weibull Life Distribution Model based on the symptom Y (e.g. crack width) caused by the damage parameter X (e.g. average corrosion penetration rate), its probability density function (PDF) is defined as [35]:

$$f(Y) = (\frac{\alpha}{Y})\left(\frac{Y}{Y_b}\right)^{\alpha} \exp(-\left(\frac{Y}{Y_b}\right)^{\alpha}) \tag{17}$$

Where $Y_b = \gamma Y_L$ and γ is the scale factor, calculated from the design requirements and the limit value of Y_L. The value of the shape factor (0 <α) is calculated by the following formula [35]:

$$\alpha = \frac{\sum_i \{\ln\left[-\ln\left(1-\frac{x_i}{x_b}\right)\right]\}^2}{\sum_i \left\{\ln\left[-\ln\left(1-\frac{x_i}{x_b}\right)\right]\right\}\ln(\frac{Y_i}{Y_b})} \tag{18}$$

The damage parameter x_b corresponds to Y_b. The probability of failure (cumulative distribution function CDF) is expressed as a function of damage parameter $x_{(t)}$ with respect to time t as follows [35].

$$P_f(Y(t)) = 1 - \exp[-\left(\frac{Y(t)}{Y_b}\right)^{\alpha}] \tag{19}$$

By calculating probability of failure, the reliability based on symptom (survival function) for the symptom Y is expressed as a function of damage parameter $x_{(t)}$ as follows [35]:

$$R(Y(t)) = \int_{Y(t)}^{\infty} f(y)dy = \exp[-\left(\frac{Y(t)}{Y_b}\right)^{\alpha}] \tag{20}$$

3.1. Bayesian Theory and Reliability

In 1958, Bayesian theory was first developed by Thomas Bayes. This method is used for adjusting previous information to new evidence in order to update or modify studied parameters. In maintenance studies,

routine inspections, maintenance and repairs are conducted to update information on the structures and make decisions about their future. This information should be considered in probabilistic functions and service life.

Under such conditions, when the structure is monitored, inspected, or repaired at the specific crack width $\widetilde{w} = \widetilde{w}^a$, the entire structure undergoes some changes in reliability and probability of failure. Therefore, the crack width information must be updated. The function $g(\widetilde{w}.\widetilde{w}^a)$ is defined as a likelihood function to simulate up-to-date values [35]:

$$g(\widetilde{w}.\widetilde{w}^a) = f(\widetilde{w} - \widetilde{w}^a) = \frac{\alpha}{\widetilde{w} - \widetilde{w}^a}\left(\frac{\widetilde{w} - \widetilde{w}^a}{\lambda' w_l}\right)^{\alpha} \exp[-\left(\frac{\widetilde{w} - \widetilde{w}^a}{\lambda' w_l}\right)^{\alpha}] \tag{21}$$

In this equation, λ' is the scale factor updated and represented as follows [35]:

$$\lambda' = \frac{w^a}{w_l}[-\ln\left(1 - \frac{\bar{x}^a}{\bar{x}_b}\right)]^{-1/\alpha} \tag{22}$$

In this equation, $\bar{x}^a$ is the average corrosion penetration rate at the crack width $\widetilde{w}^a$. Having been updated, probability density function must be multiplied by the reliability symptom $\widetilde{w} = \widetilde{w}^a$, $R(\widetilde{w}^a)$ to keep the unity of cumulative distribution function. Accordingly, at different crack widths $\widetilde{w} = \widetilde{w}_i^a$, the probability density function is expressed as [36]:

$$f_{i+1}^a(\widetilde{w}) = \frac{g_i(\widetilde{w}.\widetilde{w}_i^a) f_i(\widetilde{w})}{\int_0^{\infty} g_i(\widetilde{w}.\widetilde{w}_i^a) f_i(\widetilde{w}) d\widetilde{w}} R_i(\widetilde{w}_i^a) \tag{23}$$

The $g_i(\widetilde{w}.\widetilde{w}_i^a)$ is the likelihood function of i-th structure assessment program at the crack width $\widetilde{w} = \widetilde{w}_i^a$ and $f_i(\widetilde{w})$ is the initial probability density function for structure assessment. $R_i(\widetilde{w}_i^a)$ shows the structural reliability of i-th structure assessment program [36].

Therefore, the reliability is obtained via integration of updated probability density function over the desired point [36]:

$$R^a(\widetilde{w}) = \int_{\widetilde{w}}^{\infty} f^a(\theta)d\theta \tag{24}$$

In general, repairs are necessary for structure safety improving its strength and reliability. After repairs, the symptom-based reliability profile is changed. The probability density function in the crack width $\widetilde{w} = \widetilde{w}_j^r$ after repairs is modified as [37]:

$$f_{j+1}^r(\widetilde{w}) = f(\widetilde{w}) \quad for\ \widetilde{w} < \widetilde{w}_j^r$$
$$f_{j+1}^r(\widetilde{w}) = f_j(\widetilde{w} - \widetilde{w}_j^r) R_j(\widetilde{w}_j^r)\ for\ \widetilde{w}_j^r \leq \widetilde{w} < \widetilde{w}_{j+1}^r \tag{25}$$

3.2. Sample Modeling

A sample beam is tested in the marine environment. The beam profile specifications are described in Section 2.3. The predicted data on crack growth are analyzed in three different modes to model the sample beam in the probability distribution function. In the first step, the structure is inspected without repair and maintenance. The structure surface is then inspected at a crack width of 0.8 mm. In the third step, beam repairs are made at a crack width of 1.2 mm. In the fourth step, the beam surface is inspected at a crack width of 0.8 mm and the structure is repaired at a crack width of 1.2. Finally, the probability of failure and the reliability of structure are examined. In fact, the structure is inspected after observing 0.8 mm wide cracks on the concrete surface. This inspection leads to structural modification. Later, at another time in the structure life cycle, repairs are made at a 1.2 mm width of cracks. The state (remaining life) of the structure changes after making repairs and inspections. Providing updates and information on the structure is thus necessary to re-predict the remnant life of the structure. In this case, the structure is updated using Bayesian theory.

Figure 4 shows the structure probability density as a function of crack width. According to the initial state of the structure without maintenance and repairs, there is 50% probability of failure at the crack width of 1 mm. This state represents a structure working on all the basic engineering assumptions of 60-year life expectancy. After conducting inspection and updating information on the structure state, a tangible change occurs in the density function. According to the cumulative distribution function shown as a function of crack width (Figure 5), the structure operates on less than 40% probability of failure at the crack width of 1 mm. When the structure is inspected at the crack width of 0.8 mm, there is a sudden fall in the structural deterioration process continuing on a slower rate.

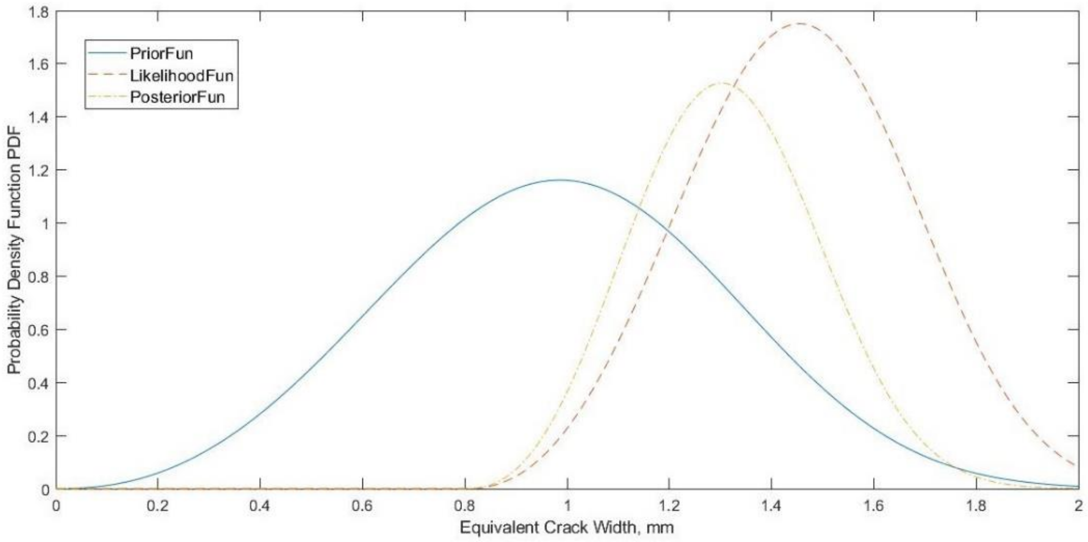

Figure 4. The initial, likelihood, and future probability density functions at 0.8 crack width inspection

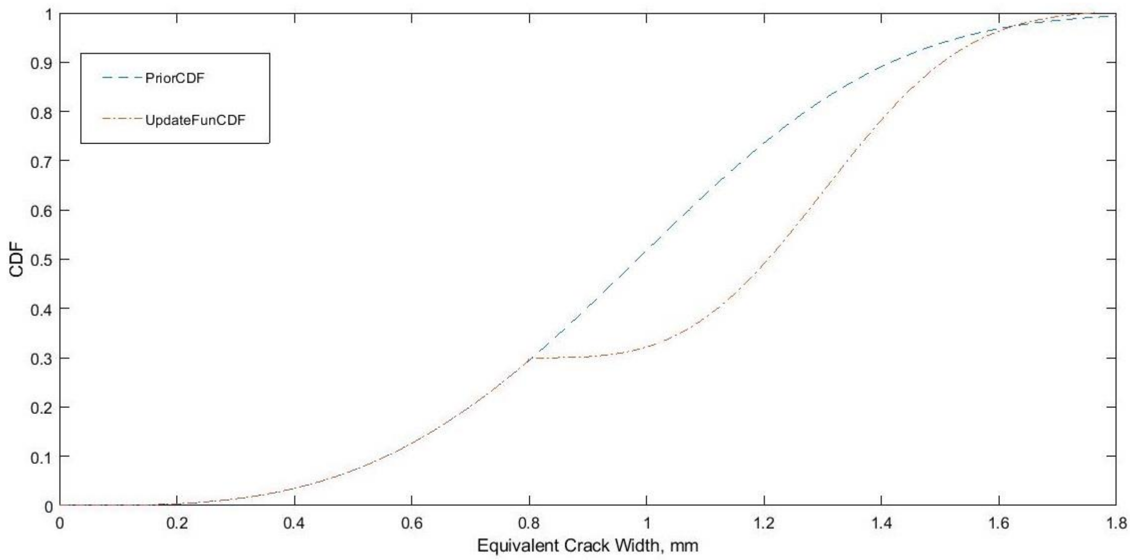

Figure 5. The diagram of cumulative distribution function for the structure both without and with inspection at the crack width of 0.8 mm

In the third step, the structure is modeled in such a way that repairs are conducted on the structure only at a crack width of 1.2 mm. There is more than 50 % probability of failure at the crack width of 1.2 before repairs, which is sharply reduced afterward. By making repairs, the probability density function and the probability of failure reach near zero at a crack width of 0.3 mm (shown in Figures 6 and 7). Therefore, repairs affect the process of structural deterioration. The probability of failure is procrastinated from 2 mm to more than 2.5 mm crack width in the structure.

In the fourth step of modeling, the structure is inspected at 0.8 mm and repaired at 1.2 mm crack width. In this mode, there are significant changes in the lifespan of the structure (Figure 6). The results on the probability density function from Figure 6 and the results on the probability of structural failure from Figure 7 show significant improvement in the structural reliability. In this step, there is an increase up to 2.5 mm in the structure lifespan alongside a 50% probability of failure at 1.5 mm crack width.

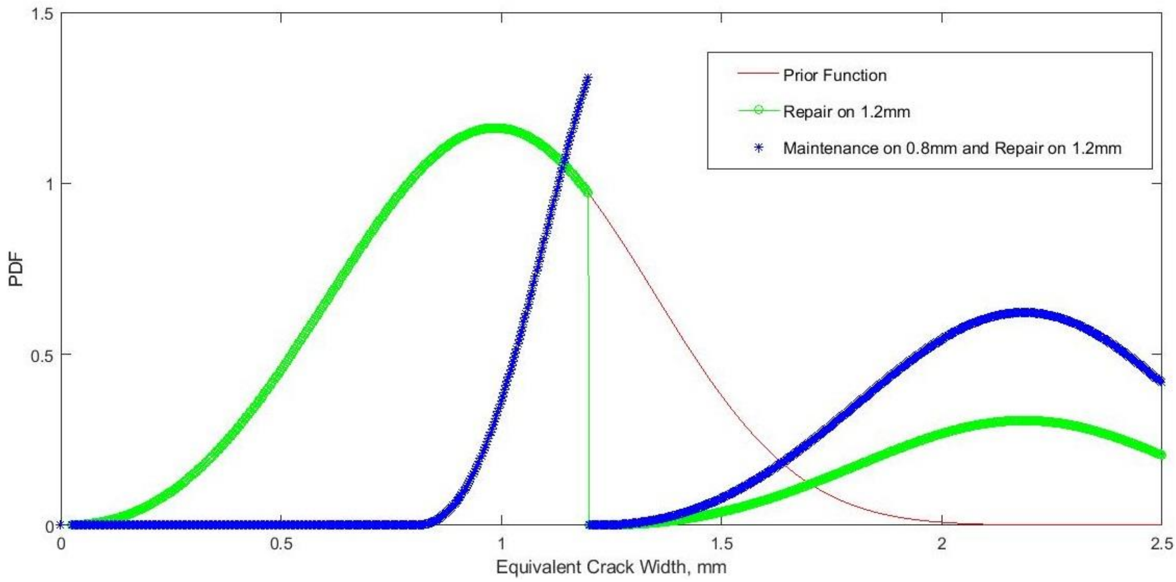

Figure 6. The probability density function under different conditions (without inspection and repairs, repairs at 1.2, inspection at 0.8, and repairs at 1.2 mm crack width)

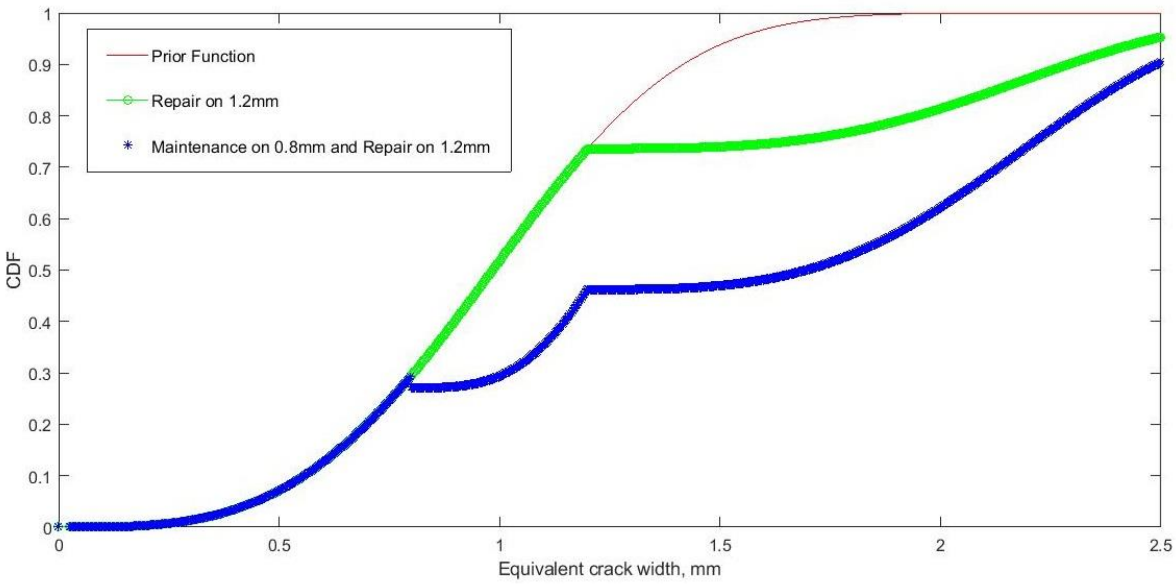

Figure 7. The probability of failure under different conditions (without inspection and repairs, repairs at 1.2, inspection at 0.8, and repairs at 1.2 mm crack width)

As expected, conducted inspections and repairs increased reliability and decreased probability of failure in the structure. As a consequence, the structure design life and durability are enhanced. Inspection, maintenance, and repair routines demand high costs. Whether maintenance implementation is a more cost-effective way than structural reconstruction is the key question. To what extent and when maintenance strategies are worth implementing and budgeting are discussed in the following.

4. Maintenance Strategy

The reliability assessment and cost analysis of the structures provide vital information for decision-making on rational management [35]. The optimal planning for making inspection, maintenance and repairs on engineering structures is conditional to cost analysis of the structure life cycle. This optimization entails minimizing the total cost of life expectancy including inspection, monitoring, maintenance, and repairs [35]. All the expected costs for the structure remaining life are expressed as [35,36]:

$$C_{total} = C_{insp} + C_{main} + C_{rep} + C_{fail} + C_{mon} \quad (26)$$

In this equation, C_{insp} expresses the inspection cost, C_{main} denotes the maintenance cost, C_{req} implies the cost of repairs, C_{fail} corresponds to the probability of failure cost, C_{mon} is the cost of monitoring the structure. The expected C_{insp} inspection costs for N_i number of inspections within the structure remaining service life of T can be calculated by Eq.(27). [35,36]:

$$C_{insp}(T) = \sum_{i=1}^{N_i} \frac{C_{insp.i}}{(1+d_r)^{t_i}} \quad (27)$$

In this equation, C_{insp} implies the cost of i-th inspection of the structure at the time t_i and d_r is the annual discount rate.
The expected maintenance cost of C_{main}, including the cost of preventive and routine maintenance over the remaining service life of T, depends on the relevant planning. The expected repair cost of C_{req} for the N_j number of repairs over the remaining service life of T is defined as [35,36]:

$$C_{rep}(T) = \sum_{j=1}^{N_j} \frac{C_{rep.j}}{(1+d_r)^{t_j}} \quad (28)$$

Where $C_{rep,j}$ is the cost of j-th repair of the structure at the time t_j.
The maintenance strategy, including inspection and repairs on the structure, may change the probability of structural failure. The cost of expected failure C_{fail} for the remaining service life of T is defined as [35,36]:

$$C_{fail}(T) = C_f P_f(0) + \sum_{t=1}^{T} \frac{C_f(P_f(t) - P_f(t-1))}{(1+d_r)^t} \quad (29)$$

Where C_f is the cost of structural failure at the present time, and $P_f(0)$ and $P_f(t)$ are the probability of failure in recent and t years, respectively.
In the case of no structural health monitoring, optimal planning is obtained from the minimization of both inspection and structural failure cost functions at the end of the structure service life T. Based on these two objective functions, minimization should be done as follows [35,36]:

$$Min\ C_{insp}(T)\ and\ Min\ C_{fail}(T) \quad (30)$$

In the case of inspection and repairs, structural information as well as reliability is updated. The repair and monitoring costs are also included in the total cost at the end of service life T. The minimization is obtained from the following objective functions [35,36]:

$$Min\ [C_{rep}(T) + C_{insp}(T)] and\ Min\ C_{fail} \quad (31)$$

Due to lack of information, the maintenance cost of the studied structure in the sea environment is assumed to be similar to that of the real structure in the corrosive environment of Orcesi and Frangopol's study [36]. Accordingly, the inspection and repair costs in different conditions are as follows.
First of all, no repair is conducted and the structure remains unchanged to the end of service life. In this step, there is no charge of maintenance. In the second step, a charge of $ 225,600 is assumed depending on the maintenance work. The charges of $229,200, $341,800, and $487,100 are considered for maintenance in the third, fourth, and fifth steps proportionate to the required repairs.
Given the definition of multi-objective optimization, inspection, repair, and failure cost functions constitute objective functions in this problem. The objective functions are identified by equations 30 and 31. The Non-dominated Sorting Genetic Algorithm (NSGA II) is used to find the best solution to the problem while optimizing the two objective functions. The design parameters of this problem include the time of maintenance and the type of selective reaction. In the first step, it is assumed that the structure is inspected at a crack width of 0.8 mm. The two objective functions are changing. The first is the inspection cost function with a different condition in the structure. The second objective function is the probability of structural failure for inspection at the crack width of 0.8 mm (Figure 5). Among various conditions, the optimal costs concerning structural failure and inspection cost functions are represented in Figure 8. According to the available budget, risk-taking potential is determined by making the best decision among the proposed selections.

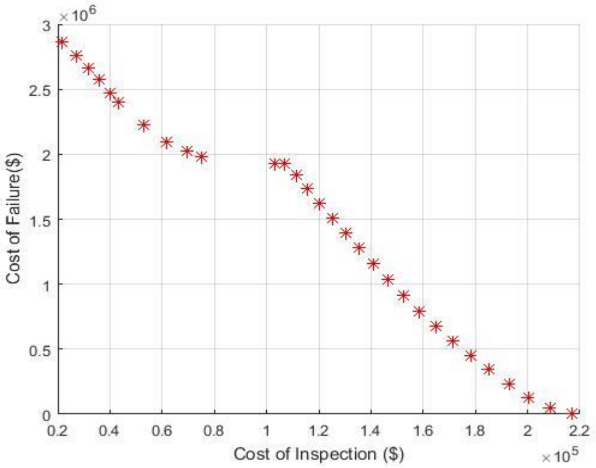

Figure 8. Pareto front diagram of the inspection cost function versus the failure cost function (with the assumption of 0.8 mm crack width)

It is further assumed that the structure is not inspected and only repaired at the crack width of 1.2 mm. In this step, the objective functions include the cost of structural failure at the crack width of 1.2 mm (Figure 7) and the cost of repairs in different modes. The best possible time and the lowest probable cost are found regarding the reliability of the structure. Figure 9 represents the resulting Pareto front including the best options for implementing structural repairs based on the crack width and the repair cost.

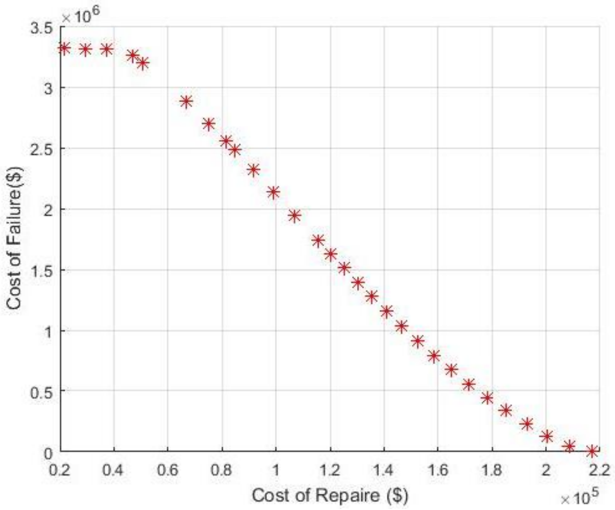

Figure 9. Pareto front diagram of repair cost function versus failure cost function (with the assumption of 1.2 mm crack width)

As seen in Figure 6, making repairs on the structure is much more effective than carrying out inspections. In fact, the reliability of the structure is increased by 0.8 mm after repairs. Assuming that a failure cost of $ 2 million is decided and comparing diagrams 9 and 10, a difference of $ 40,000 is obtained between inspection and repair costs. Making decisions on the time and the type of inspections is subject to the project budget and the employer's selection.

In the third step, the structure goes under inspection and repairs. Compared to previous steps, the probability of structural failure undergoes dramatic changes, making it extremely difficult to decide on the exact time and cost. In this case, the first function is the cost of repair and maintenance and the second function is the probability of failure considering crack width of 0.8 mm for inspection and crack width of 1.2 mm for repair (Figure 7). The best decisions are proposed using the genetic algorithm (NSGA II method) (Figure 10). The employer is provided with options relative to the potential for taking risks and the budget available.

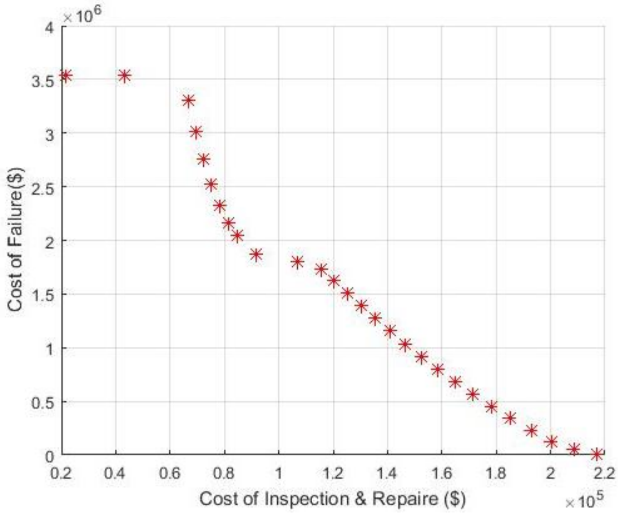

Figure 10. Pareto front diagram of inspection and repair cost function versus failure cost function (with the assumption of 0.8 mm crack width for inspection and 1.2 mm crack width for repair)

This diagram indicates that the difference between inspection and repair costs is not significant assuming that the failure cost of $ 2 million is accepted. Hence, the employer's decision on the inspection, maintenance, and repair costs is vital to take risks of structural failure.

5. Conclusions

In this paper, the propagation of crack width for a RC structure in the marine environment was investigated using Weibull probability function. The probability of failure was assessed before and after maintenance to predict the appropriate time for its implementation using Bayesian theory. The optimal condition for the structure was estimated by two functions of probability of failure and maintenance strategy. The following results are obtained:

1- Crack width was a good symptom for reliability assessment in the structure. Weibull distribution function was used to predict structural performance on the base of crack width propagation.

2- Bayesian theory and maintenance strategy were applied to update the structure information and improve its life service. The reliability and probability of failure were strongly influenced by maintenance implementation.
3- Repair and maintenance planning provided updates on the structure life expectancy and caused effects on the probability of failure and the probability density functions. The genetic algorithm (NSGA II) was used to propose the optimum strategy for repair and maintenance regarding two objective functions (probability of failure and varied strategies). It was concluded that the time and type of maintenance strategy depend on the risk-taking and financial potentials.
4- In this work, crack width propagation was the mere factor considered as a symptom. Not only may other factors affect the probability of structural failure, but also the cost of maintenance and repairs.
5- The maintenance and repairs were conducted on a fractured structure in this study. Preventive maintenance services can be investigated in future studies.

6. References

[1] Frangopol DM, Okasha NM. Life-cycle framework for maintenance , monitoring , and reliability of naval ship structures. Integration The Vlsi Journal 2010:69–76.
[2] Torres-Acosta AA, Navarro-Gutierrez S, Terán-Guillén J. Residual flexure capacity of corroded reinforced concrete beams. Engineering Structures 2007;29:1145–52. doi:10.1016/j.engstruct.2006.07.018.
[3] Li C-Q, Zheng J-J. Analytical Model for Corrosion-Induced Crack Width in Reinforced Concrete Structures. Structural Journal 2006;103:479–87. doi:10.14359/16423.
[4] Alonso C, Andrade C, Rodriguez J, Diez JM. Factors controlling cracking of concrete affected by reinforcement corrosion. Materials and Structures 1998;31:435–41. doi:10.1007/BF02480466.
[5] Y. Liu, R. E. Weyers. Modeling the Time to Corrosion Cracking in Chloride contaminated Reinforced Concrete Structures. ACI Materials Journal 1998;95:675–80. doi:10.1016/S0008-8846(98)00259-2.
[6] Andrade C, Alonso C, Molina FJ. Cover cracking as a function of bar corrosion: Part I-Experimental test. Materials and Structures 1993;26:453–64. doi:10.1007/BF02472805.
[7] Oh BH, Kim KH, Jang BS. Critical corrosion amount to cause cracking of reinforced concrete structures. ACI Materials Journal 2009;106:333.
[8] Uddin F, Maalej M, Mihashi H. Cover Cracking of Reinforced Concrete Beams Due to Corrosion of Steel 2008:2008.
[9] Chen D, Mahadevan S. Chloride-induced reinforcement corrosion and concrete cracking simulation 2008;30:227–38. doi:10.1016/j.cemconcomp.2006.10.007
[10] Barlowt P, Bartht F, Bishara AG, Boggs HL, Brandee ME, Darwin D, et al. Causes, Evaluation and Repair of Cracks in Concrete Structures 1998;93:1–22.
[11] Jayasuriya A, Pheeraphan T, Stage APS. Prediction of Time to Crack Reinforced Concrete by Chloride Induced Corrosion 2017;11:1197–203.
[12] Kirkpatrick TJ, Weyers RE, Anderson-cook CM, Sprinkel MM. Probabilistic model for the chloride-induced corrosion service life of bridge decks 2002;32:1943–60.
[13] Suo Q, Stewart MG. Corrosion cracking prediction updating of deteriorating RC structures using inspection information. Reliability Engineering and System Safety 2009;94:1340–8. doi:10.1016/j.ress.2009.02.011.
[14] Thoft-christensen P. Aalborg Universitet Papers, volume 5 - 1997-2000 Thoft-Christensen, Palle 2006;5.
[15] Ã DVV, Trapper PA. Probabilistic evaluation of initiation time of chloride-induced corrosion 2008;93:364–72. doi:10.1016/j.ress.2006.12.010.
[16] Adeli H, Sarma KC. Cost optimization of structures: fuzzy logic, genetic algorithms, and parallel computing. John Wiley & Sons; 2006.
[17] Frangopol DM, m. ASCE, Curley JP. EFFECTS OF DAMAGE AND REDUNDANCY ON STRUCTURAL RELIABILITY 3 By Dan M, Frangopol, 1 M. ASCE, and James P. Curley 2 1987;113:1533–49.
[18] CEMPEL C, NATKE HG, YAO JTP. Symptom Reliability and Hazard for Systems Condition Monitoring. Mechanical Systems and Signal Processing 2000;14:495–505. doi:10.1006/mssp.1999.1246.
[19] Straub D. Reliability updating with inspection and monitoring data in deteriorating reinforced concrete slabs. Applications of Statistics and Probability in Civil Engineering -Proceedings of the 11th International Conference on Applications of Statistics and Probability in Civil Engineering 2011:2309–16.
[20] Alani AM, Chen H-P. Reliability and optimised maintenance for sea defences. Proceedings of the ICE - Maritime Engineering 2012;165:51–64. doi:10.1680/maen.2010.37.
[21] Yu B, Ning C, Li B. Probabilistic durability assessment of concrete structures in marine environments: Reliability and sensitivity analysis. China Ocean Engineering 2017;31:63–73.
[22] Pedeferri P, Bertolini L, Elsener B, Redaelli E, Polder RB, Pedeferri P, et al. Corrosion of Steel in Concrete - Prevention, Diagnosis, Repair. 2013. doi:10.1002/3527603379.
[23] Nepal J, Chen H-P. Risk-based optimum repair planning of corroded reinforced concrete structures. Structural Monitoring and Maintenance 2015;2:133–43. doi:10.12989/smm.2015.2.2.133.
[24] Chen H. Monitoring-Based Reliability Analysis of Aging Concrete Structures by Bayesian Updating 2015:1–8. doi:10.1061/(ASCE)AS.1943-5525.
[25] Law DW, Tang D, Molyneaux TKC, Gravina R. Impact of crack width on bond: Confined and

unconfined rebar. Materials and Structures/Materiaux et Constructions 2011;44:1287–96. doi:10.1617/s11527-010-9700-y.

[26] Nepal J, Chen H. Risk-based optimum repair planning of corroded reinforced concrete structures. Structural Monitoring and Maintenance 2015;2:133–43. doi:10.12989/smm.2015.2.2.133.

[27] Zhang R, Castel A, François R. Concrete cover cracking with reinforcement corrosion of RC beam during chloride-induced corrosion process. Cement and Concrete Research 2010;40:415–25. doi:10.1016/j.cemconres.2009.09.026.

[28] Chen H, Alani AM. Optimized maintenance strategy for concrete structures affected by cracking due to reinforcement corrosion. ACI Structural Journal 2013;110:229–38.

[29] Bazant ZP, Planas J. Fracture and size effect in concrete and other quasibrittle materials. vol. 16. CRC press; 1997.

[30] Hillerborg A, Modéer M, Petersson PE. Analysis of crack formation and crack growth in concrete by means of fracture mechanics and finite elements. Cement and Concrete Research 1976;6:773–81. doi:10.1016/0008-8846(76)90007-7.

[31] Zhang R, Castel a., François R. Serviceability Limit State criteria based on steel–concrete bond loss for corroded reinforced concrete in chloride environment. Materials and Structures 2009;42:1407–21. doi:10.1617/s11527-008-9460-0.

[32] Torres-Acosta AA, Sagues AA. Concrete cracking by localized steel corrosion--Geometric effects. Materials Journal 2004;101:501–7.

[33] Torres-Acosta A a., Mart nez-Madrid M. Residual Life of Corroding Reinforced Concrete Structures in Marine Environment. Journal of Materials in Civil Engineering 2003;15:344–53. doi:10.1061/(ASCE)0899-1561(2003)15:4(344).

[34] Vidal T, Castel A, François R. Analyzing crack width to predict corrosion in reinforced concrete. Cement and Concrete Research 2004;34:165–74. doi:10.1016/S0008-8846(03)00246-1.

[35] Chen H-P, Ni Y-Q. Structural Health Monitoring of Large Civil Engineering Structures. 2018. doi:10.1002/9781119166641.

[36] Orcesi AD, Frangopol DM. Optimization of bridge maintenance strategies based on structural health monitoring information. Structural Safety 2011;33:26–41. doi:10.1016/j.strusafe.2010.05.002.

[37] Okasha NM, Frangopol DM. Lifetime-oriented multi-objective optimization of structural maintenance considering system reliability, redundancy and life-cycle cost using GA. Structural Safety 2009;31:460–74. doi:10.1016/j.strusafe.2009.06.005.